Supporting Information

Surface-alkalinization-induced enhancement of photocatalytic H_2 evolution over $SrTiO_3$-based photocatalysts

Authors:

Shuxin Ouyang,[1] Hua Tong,[2,3] Naoto Umezawa,[1,3,4] Junyu Cao,[1] Peng Li,[1,2] Yingpu Bi,[2] Yuanjian Zhang,[2] and Jinhua Ye[*,1,2,3]

[1] *Environmental Remediation Materials Unit, National Institute for Materials Science (NIMS), 1-2-1 Sengen, Tsukuba, Ibaraki 305-0047, Japan*

[2] *International Center for Materials Nanoarchitectonics (WPI-MANA), National Institute for Materials Science (NIMS), 1-2-1 Sengen, Tsukuba, Ibaraki 305-0047, Japan*

[3] *TU-NIMS Joint Research Center, School of Materials Science and Engineering, Tianjin University, 92 Weijin Road, Nankai District, Tianjin, P.R. China*

[4] *PRESTO, Japan Science and Technology Agency (JST), 4-1-8 Honcho Kawaguchi, Saitama 332-0012, Japan*

[*] Author to whom correspondence should be addressed.

Electronic mail: jinhua.ye@nims.go.jp.

SI-1 Experimental and Calculational Procedures

1. Synthesis of STO and La,Cr-STO Powders

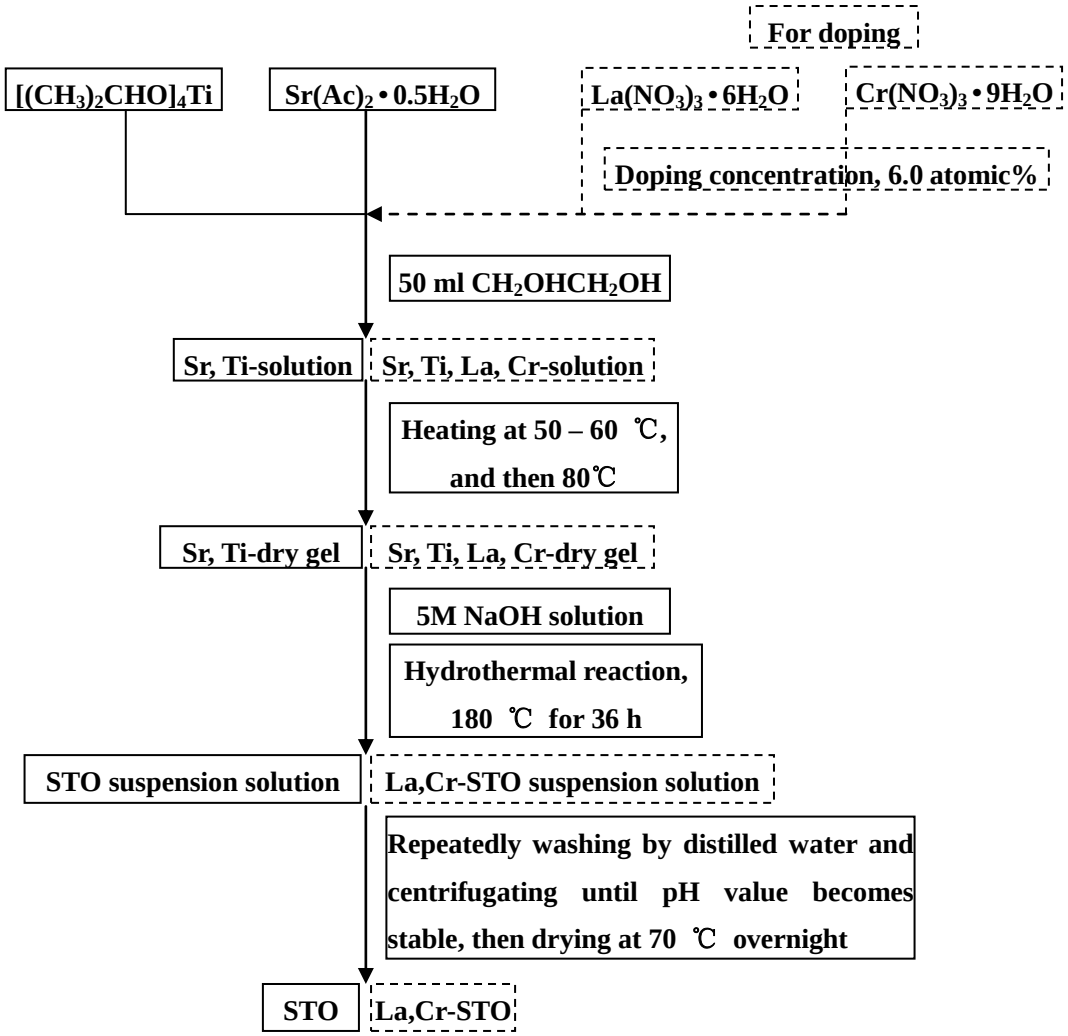

Figure S1. Flowchart of the preparation of STO and La,Cr-STO powders

2. **Characterizations**

Structural features of the specimens were determined using powder X-ray diffraction (RINT-2000; Rigaku Corp., Japan) with Cu $K\alpha_1$ radiation. The diffuse reflectance spectra of the samples were recorded on a UV-visible spectrophotometer (UV-2500PC; Shimadzu Corp., Japan) with barium sulfate as the reference. Then the absorption spectra were obtained from the reflectance spectra by means of Kubelka–Munk transformations. Morphology observation and qualitative analysis for the elemental compositions were performed using a high-resolution transmission electron microscope (JEM 2010; JEOL Corp., Japan; operated at 200 kV). The Brunauer–Emmett–Teller (BET) surface areas were measured via nitrogen physisorption (Gemini2360; Micromeretics Corp., U.S.A.).

3. Photocatalytic Reactions

The photocatalytic H_2 evolution was carried out with 0.3 g photocatalyst (loading 0.5 wt% Pt as cocatalyst by photodeposition) suspending in 270 ml CH_3OH solution (50 ml CH_3OH and 220 ml H_2O) in a Pyrex glass reaction cell. The alkalinity of solution was adjusted by adding NaOH pills. The reaction cell was connected to a gas-closed system with a gas-circulated pump. A 300-W Xe arc lamp was employed for the light source of photocatalytic reaction. During the visible-light reaction, a L42 cutoff filter was used to remove UV light ($\lambda > 400$ nm). In the cases of the measurement of apparent quantum efficiency (*AQE*), 382 nm band-pass filter and 420 nm band-pass filter + L42 cutoff filter were used to produce monochromatic light. The intensity of incident light was measured by a spectroradiometer (Ushio, USR-40, Japan). The evolved H_2 was analyzed by an online gas chromatograph (GC-8A; Shimadzu Corp., Japan) equipped with a thermal conductivity detector. The apparent quantum efficiency was calculated as following equation,

$$AQE = N(H_2) \times 2 / N(Photons) \times 100\%$$

in which $N(H_2)$ and $N(Photons)$ signify the molecular number of generated H_2 in unit time and the number of incident photons in unit time, respectively.

4. Photoelectrochemical Measurements

The $SrTiO_3$ electrode was prepared by a spin coating method. The commercial $SrTiO_3$ (nano-sized, Wako, Japan) was prepared to be a gel in ethanol with a concentration of 7.1 μmol/ml. The gel was spin-coated on an ITO substrate with a rate of 1000 rpm for 30 s. This process was repeated for 50 times. Then, the thin film was sintered at 400℃ for 2 h. Photoelectrochemical properties were measured in a three-electrode configuration equipped with a Ag/AgCl reference electrode. The electrolyte was a solution of 20:80 CH_3OH and distilled water. The alkalinity of electrolyte was adjusted by adding NaOH pills. Platinum wire worked as counter electrode. Schematic illustration of the test system was plotted as below.

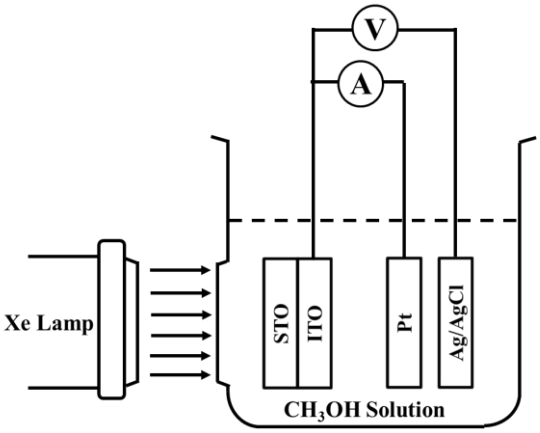

Figure S2. Schematic configuration of the setup of two-electrode photoelectrochemical measurement

In order to well simulate the photocatalytic process, the measurement of photocurrent change vs pH value was performed under 0 V bias potential. The open-circuit potential and closed-circuit potential were also measured. Although the open-circuit potential indicates the difference of electrical potential between the STO electrode and the counter electrode (or the reaction solution), it just reflects a static condition. The closed-circuit potential can reveal the dynamic case of photocatalytic reaction (the whole photocatalytic reaction is a kind of redox cycle). Actually, both the closed-circuit potential and open-circuit potential changes vs pH value show the same trend, exponential relation (as exhibited in following figure).

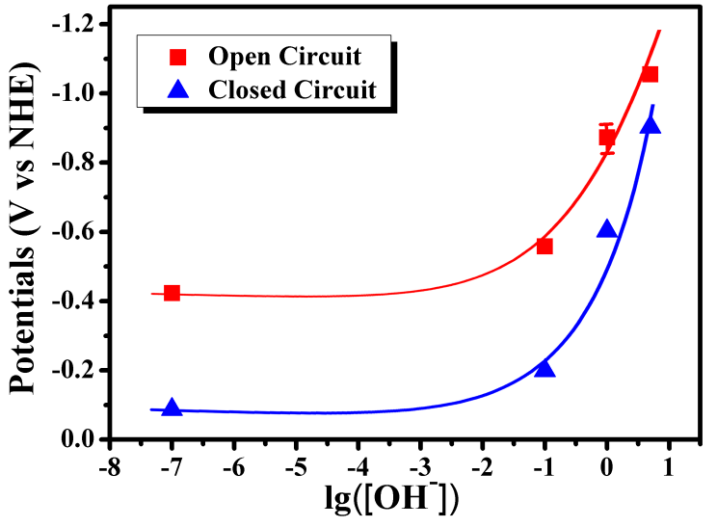

Figure S3. The closed-circuit potential and open-circuit potential changes versus pH value.

5. Characterizations of Photoinduced Hydrophilicity

The $SrTiO_3$ thin film prepared by the spin-coating technique was also used to test the photoinduced hydrophilicity. In a typical process, the thin film was soaked in a solution with 20 ml CH_3OH and 80 ml distilled water under UV-visible light irradiation for 10 min. The alkalinity of solution was also adjusted by NaOH pills. After irradiation, the thin film was cleaned by distilled water for 1 min and dried by N_2 gas to remove liquid water, and then dried in oven for 30 min to eliminate most of adsorbed gaseous water. After that, when the thin film was cooled down to room temperature, the measurements of contact angle was performed. We tested 5 – 7 different positions on one film. The highest and lowest values of contact angle were ignored, and the other values were used to calculate the average.

6. Calculations on Surface Electronic Structures of $SrTiO_3$

Our electronic structure calculations were based on the density-functional theory (DFT) + *U*

approach.[1] The exchange-correlation energy functional was represented by the local density approximation (LDA) proposed.[2] Projector-augmented wave pseudopotentials were employed as implemented in the VASP code.[3,4] The valence configurations of the pseudo-potentials were $4s^2 4p^6 5s^2$ for Sr, $3p^6 3d^3 4s^1$ for Ti and $2s^2 2p^4$ for O. The energy cutoff for the plane-wave basis set expansion was set at 500 eV. A Monkhorst-Pack k-point sets of $6\times6\times6$ was used for a 5-atom unit cell of cubic $SrTiO_3$ (space group $Pm\bar{3}m$). We applied U to Ti d and O p (U(Ti d) = 9.14 eV and U(O p)=5.32 eV) which were determined so as to reproduce the experimental band gap (3.2 eV).[5] The importance of applying U to O p as well as Ti d states was discussed elsewhere.[6] The 5-atom unit cell was fully relaxed for atomic positions and cell volume. The optimized lattice constant (3.92 Å) is in good agreement with an experimental value (3.905 Å).[7]

The relaxed unit cell was extended to construct the surface models shown in Fig. S4. Oxygen terminated non-polar (110) surface was created with ten SrTiO layers and 10 Å of vacuum region which results in a 50-atom slab model. The mid layers (5th and 6th layers) of the slab were fixed during geometry relaxations in order to represent a bulk region. We firstly removed two electrons from the ideal surface to investigate the effects of hole carriers (h^+). The surface geometry is largely reconstructed from the bulk configuration as shown in Fig. S4a where the slab is extended by 3×3 in the planar direction and only one side of the slab is depicted for the visualization purpose. This model is denoted as [(110) + h^+] in the following. The introduction of OH^- on the surface stabilizes the system because it helps terminating metal atoms; each O atom from OH^- forms bonds with two Sr and one Ti atoms on the surface as shown in Fig. S4b. This model, which is called [(110) + h^+ + OH^-], represents a surface in a high pH environment in our computational results. The density of states (DOS) of each model is shown in Fig. S5. Here, the origin of the horizontal axis is calibrated for aligning the averaged electrostatic potential in the fixed layers (V_{av}) with respect to that of the ideal surface in a neutral charge state. It is clearly shown that both the valence and conduction band edges are higher in [(110) + h^+ + OH^-] than in [(110) + h^+], possibly due to the neutralization of the surface. This is in good agreement with the experimental results that the Fermi level shifts upward in a high pH condition.

To further investigate the effect of the high pH environment, we have computed the surface energies of several surface structures. The surface energy is defined by the following formula,

$$\gamma = (E_{surf} - \mu_{Mol} + Q(\varepsilon_F + \varepsilon_v + \Delta V))/A,$$

$$E_{surf} = (E_{slab} - nE_{bulk})/2,$$

where E_{slab} is the total energy of the slab and E_{bulk} is the total energy of the bulk per unit. The μ_{Mol} is the chemical potential of either OH or H_2O which is estimated from the total energy of each molecule given by our DFT calculation. The ε_F is the Fermi energy with respect to the valence band maximum of the ideal surface without the hole carriers ε_v, and ΔV is the correction to ε_v for the shift in the V_{av} from that of the neutral surface due to the introduction of either the hole carriers or

adsorbate molecules. The *Q* is the charge introduced on the surface. Here, n is the number of bulk unit cells contained in the slabs (n = 10 in our models), and A is the surface area of each side of the slab (A= 21.74 $Å^2$). The results are summarized in Table S1 for two different Fermi energy conditions: ε_F = 0.0 and ε_F = 1.6 eV. In any case, [(110) + h^+ + OH^-] gives the lowest surface energy among the model structures examined, indicating OH^- is associated with a STO (110) surface under the presence of photo-induced hole carriers. This result is consistent with our experimental observations that the hydrophilicity on the STO surface is enhanced as alkalinity of the solution is increased. Note that the surface energy can be negative when a solid surface is terminated by external species.[8-10] Our computational results in Table S1, therefore, show a reasonable trend.

References

1. Anisimov, V. I.; Zaanen, J.; Andersen, O. K. *Phys. Rev. B* **1991**, *44*, 943.
2. Perdew, J. P.; Zunger, A. *Phys. Rev. B* **1981**, *23*, 5048.
3. Kresse, G.; Hafner, J. *Phys. Rev. B* **1993**, *47*, 558.
4. Kresse, G.; Furthmüller, J. *Phys. Rev. B* **1996**, *54*, 11169.
5. Benthem, K. V.; Elsasser, C.; French, R. H. *J. Appl. Phys.* **2001**, *90*, 6156.
6. Morgan, B. J.; Watson G. W. *Phys. Rev. B* **2009**, *80*, 233102.
7. Okazaki, A.; Kawaminami, M. *Mater. Res. Bull.* **1973**, *8*, 545.
8. Łodziana, Z.; Topsøe, N.-Y.; Nørskov, J. K. Nature Mater. **2004**, *3*, 289.
9. Gumbsch, P.; Daw, M. S. *Phys. Rev. B* **1991**, *44*, 3934.
10. Meade, R. D.; Vanderbilt, D. *Phys. Rev. Lett.* **1989**, *63*, 1404.

SI-2 Transmission Electron Microscope/Energy-Dispersive X-ray Measurement for La,Cr-STO

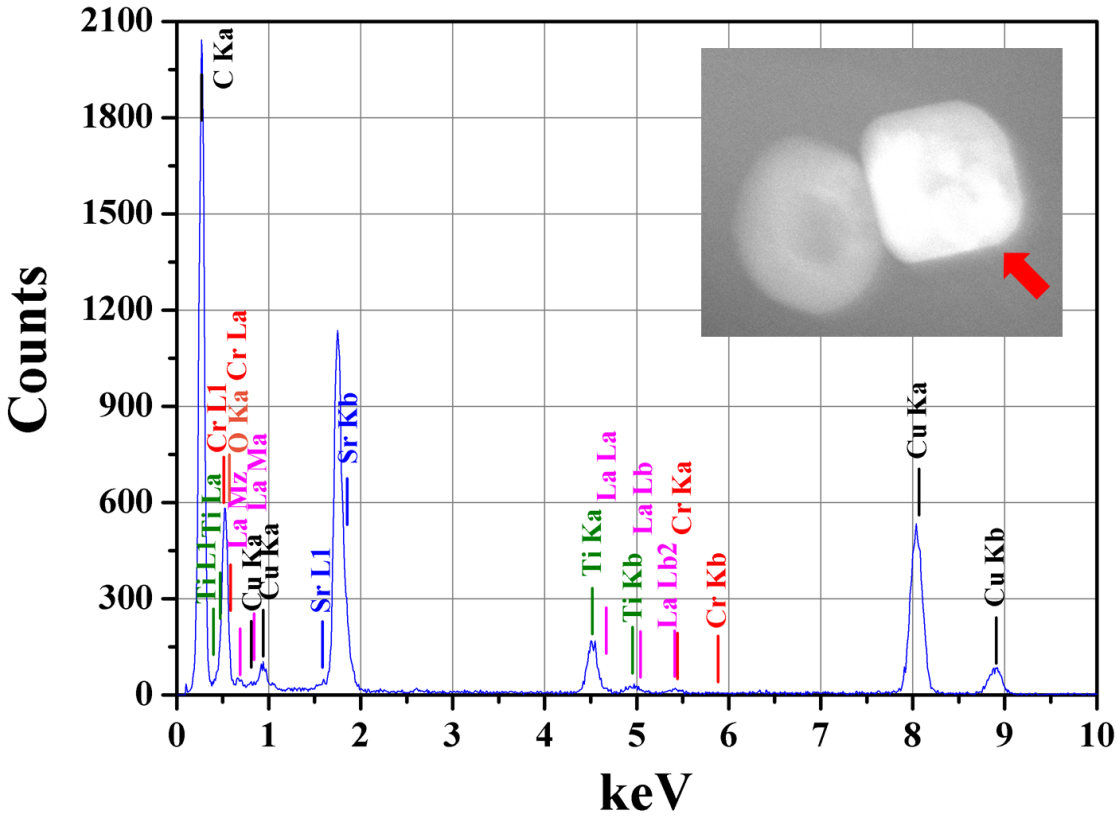

SI-3 Calculations on Surface Electronic Structures of $SrTiO_3$

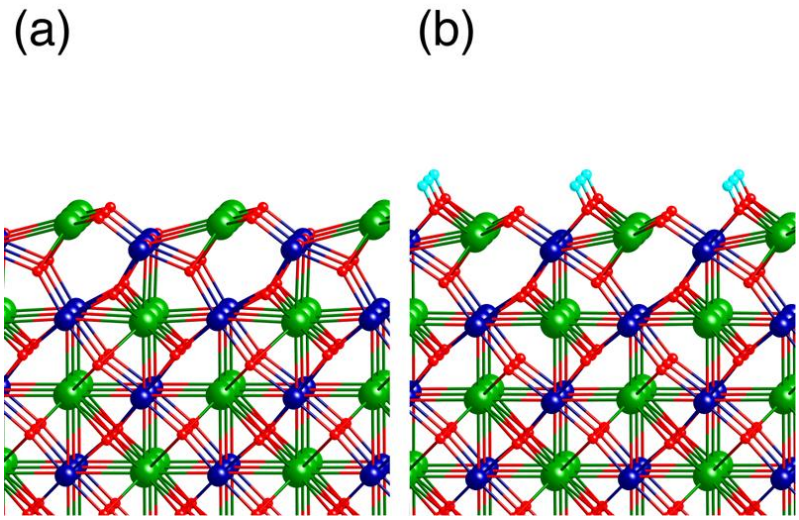

Figure S4. Relaxed geometries of the surface models based on the $SrTiO_3$ (110) facet, (a) an ideal surface with a hole carrier [(110) + h^+] and (b) OH^- adsorbed surface with a hole carrier [(110) + h^+ + OH^-]. Here, the slab is extended by 3×3 in the planar direction and only one side of the slab is depicted for the visualization purpose. The green, navy, red, and cyan particles denote the positions of Sr, Ti, O, and H atoms, respectively.

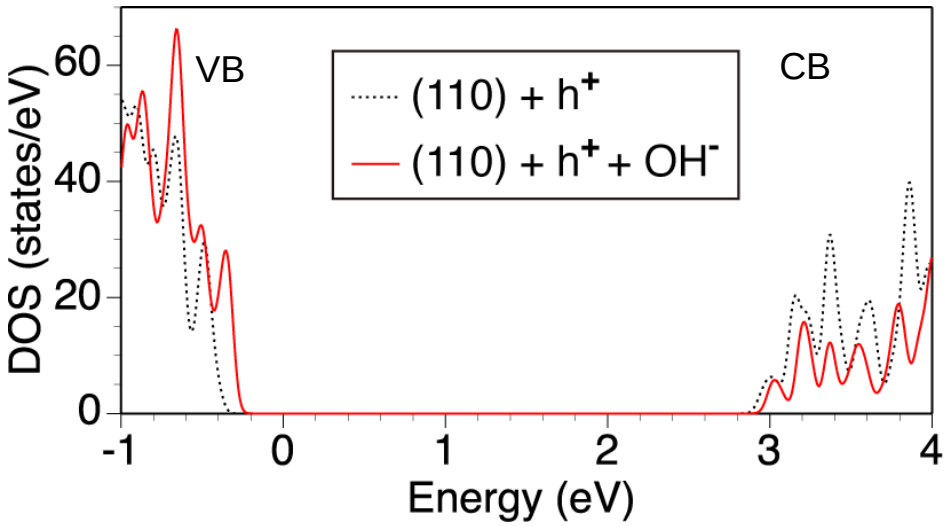

Figure S5. Total density of states for the two surface models shown in Fig. S1. The origin of the horizontal axis is calibrated for aligning the averaged electrostatic potential in the fixed layers (V_{av}) with respect to that of the ideal surface in a neutral charge state. The width of smearing was set to 0.05 eV.

Table S1. Surface energies for the relaxed model structures: the ideal surface in neutral charge state, (110), the ideal surface with a hole carrier, [(110) + h^+], the H_2O adsorbed surfaces without a hole, [(110) + H_2O], and with a hole, [(110) + h^++ H_2O], and the OH^- adsorbed surface, [(110) + h^+ + OH^-], for two different Fermi energy conditions: ε_F = 0.0 eV and ε_F = 1.6 eV.

Models	Surface Energy (ε_F = 0.0 eV,) / J•m^{-2}	Surface Energy (ε_F = 1.6 eV,) / J•m^{-2}
(110)	1.11	1.11
[(110) + h^+]	0.86	2.04
[(110) + H_2O]	-0.67	-0.67
[(110) + h^+ + H_2O]	-0.98	0.20
[(110) + h^+ + OH^-]	-1.41	-1.41

SI-4 Schematic Illustration of Alkalinity-Induced Separation of Carriers